Preprints of the 21st IFAC World Congress (Virtual)
Berlin, Germany, July 12-17, 2020

Flexible Control of Nuclear Cogeneration Plants for Balancing Intermittent Renewables

Zhe Dong*, **, Di Jiang*, Zhiwu Guo, Xiaojin Huang***

** Institute of Nuclear and New Energy Technology, Collaborative Innovation Center of Advanced Nuclear Energy Technology of China, Key Laboratory of Advanced Reactor Engineering and Safety of Ministry of Education, Tsinghua University, Beijing 100084, China (Tel: 86-10-62783764; e-mail: dongzhe@tsinghua.edu.cn).*

*** State Key Laboratory of Nuclear Power Safety Monitoring Technology and Equipment, Shenzhen, Guangdong, 518172, China.*

Abstract: Due to the complementarity between the intermittent renewable energy (IRE) and the nuclear, it is attractive to interconnect them to supply clean energy consistently and continuously in a large-scale. The flexibility of for integrating the IRE can be provided by actively adjusting the electric power output of nuclear cogeneration plants (NCPs), which induces frequent redistribution of main steam to the turbine and cogeneration process. For the main steam redistribution, it is necessary to guarantee the stability of grid frequency and main steam pressure, which heavily relies on the flexible control of NCPs. In this paper, a new flexible control of NCPs with saturated main steam is proposed based upon the idea of actively suppressing the total disturbance in the dynamics of grid frequency and that of main steam pressure. The stabilization problems of pressure and frequency are transferred to the disturbance attenuation problem of a second-order system, and an active disturbance rejection control (ADRC) is then proposed. This ADRC is applied to the flexible control of a NCP composed of a nuclear heating reactor (NHR), a turbine-generator set and a multi-effect-desalination and thermal-vapor-compression (MED-TVC) process for seawater desalination. Numerical simulation results in the cases of load stepping show that the flexibility of this NCP is satisfactory in balancing the grid.

Keywords: renewable integration, nuclear cogeneration, disturbance attenuation

1. INTRODUCTION

Although intermittent renewable energy (IRE) resources such as the wind and solar are going to make our planet a better place to live (Alizadeh, et al., 2016), however since IRE cannot provide power supply consistently and continuously, the large-scale integration of IRE may significantly aggravate the grid imbalance (Lund, et al., 2015). Actually, the integration cost has been a key part in the total cost of IRE generation [3]. With comparison to IRE, nuclear power plants (NPPs) are able to provide consistent and clean power supply with small land footprint (Kondziella and Bruckner, 2016). Nuclear power practices have been adapted over the years for balancing power supply and demand either due to the high share of nuclear in the energy mix such as France or the massive deployment of IRE in the mix such as Germany (Suman, 2018).

The flexibility of nuclear plants for grid balance can be given by either load-following or cogeneration. To provide satisfactory level of flexibility while keeping a higher load factor of nuclear reactors, cogeneration is better to be used, where the frequency fluctuation caused by IRE generation is stabilized by bypassing the excess main steam flow provided by a nuclear steam supplying system (NSSS) to the backup cogeneration processes for desalination, hydrogen production, natural gas reforming and etc. (Locatelli, et al., 2017). With comparison to the nuclear plants providing flexibility through load-following, the reactor of a nuclear cogeneration plant (NCP) is kept at a constant level, where the redistribution of main steam is given by the electric power from IRE plants (Cany, et al., 2016). Although there have already been abundant results for the load-following control of nuclear power plants (Li, et al, 2016), there is still very limited results in the flexible control of NCPs

In this paper, the flexible control of NCP is realized by stabilizing the grid frequency and main steam pressure based upon the redistribution of main steam. An active disturbance rejection control (ADRC) is proposed for the stabilization, which contains a proportional-integral feedback term and a feedforward term driven by a 3rd-order disturbance observer (DO). Then, this ADRC is applied for the flexible control of a NCP based on nuclear heating reactor for electricity generation and seawater desalination. Simulation results in the case of power stepping show that this NCP flexible controller is feasible for the grid balance in the context of deep renewable penetration.

2. MODELING AND PROBLEM FORMULATION

The control design oriented state-space models of the dynamics of main steam pressure and that of grid frequency are given, and the control problem is formulated.

2.1 State-Space model of Main Steam Pressure Error

Based on the energy conservation law, the energy balance for the secondary side of steam generators can be given by

$$V_{\mathrm{s}} \frac{\mathrm{d}}{\mathrm{d}t}\left(\rho_{\mathrm{s}} h_{\mathrm{s}}\right)=Q_{\mathrm{in}}+G_{\mathrm{fw}} h_{\mathrm{fw}}-\left(G_{\mathrm{tb}}+G_{\mathrm{co}}\right) h_{\mathrm{st}}, \quad (1)$$

where V_s is the total volume of the secondary sides of steam generators (SGs), ρ_s and h_s are respectively the average density and enthalpy of secondary coolant of steam generator (SG), Q_{in} is the heat flux from the primary to the secondary sides of SG, G_{fw} and h_{fw} are respectively the mass flowrate and enthalpy of SG feedwater, G_{tb} and G_{co} are the steam flowrates at the inlet of turbine and cogeneration process respectively, and h_{st} is the enthalpy of main steam. It is assumed that both

$$\rho_{\mathrm{s}} h_{\mathrm{s}}=\left(\rho_{\mathrm{fw}} h_{\mathrm{fw}}+\rho_{\mathrm{st}} h_{\mathrm{st}}\right) / 2, \quad (2)$$

and the product $\rho_{fw}h_{fw}$ are constant, where ρ_{fw} is the density of SG feedwater, and ρ_{st} and h_{st} are respectively the density and enthalpy of main steam. Based on this assumption, energy balance equation (1) can be rewritten as

$$\frac{V_{\mathrm{s}}}{2} \frac{\mathrm{d}}{\mathrm{d}t}\left(\rho_{\mathrm{st}} h_{\mathrm{st}}\right)=Q_{\mathrm{in}}+W_{\mathrm{fw}}\left(\rho_{\mathrm{fw}} h_{\mathrm{fw}}\right)-\left(G_{\mathrm{tb}}+G_{\mathrm{co}}\right) h_{\mathrm{st}}, \quad (3)$$

where $W_{fw}=G_{fw}/\rho_{fw}$ is volume flowrate of SG feedwater. Here, steam flows G_{tb} and G_{co} can be represented as

$$G_{\mathrm{a}}=C_{\mathrm{a}} X_{\mathrm{a}} \sqrt{\rho_{\mathrm{st}} P_{\mathrm{st}}}, \quad (4)$$

where footnote a=tb, co representing turbine-generator system and cogeneration process respectively,

$$X_{\mathrm{a}}=\sqrt{1-P_{\mathrm{a}} / P_{\mathrm{st}}}, \quad (5)$$

C_a is the conductance of flowrate control actuator such as the steam regulating valve of turbine and the ejector of MED-TVC process, P_{st} is the main steam pressure, and P_a is the pressure just after the actuator. For the turbine-generator system, since the difference between P_{st} and P_{tb} is small so as to keep the efficiency, X_{tb} is very small. For the MED-TVC process, since the pressure at the ejector throat is much lower than P_{st}, it can be seen that $X_{co}\approx 1$. Thus, it is reasonable to assume that scalar X_a (a=tb, co) are positive constants.

Furthermore, based upon the fact that the main steam is saturated as well as the assumptions that both product $\rho_{fw}h_{fw}$ and scalar X_a are constant, the error dynamics of main steam pressure can be derived from equation (3) as

$$\begin{aligned}
&\frac{V_{\mathrm{s}}}{2}\left[\left.\frac{\partial\left(\rho_{\mathrm{st}} h_{\mathrm{st}}\right)}{\partial P_{\mathrm{st}}}\right|_{P_{\mathrm{st0}}}\right] \frac{\mathrm{d} \Delta P_{\mathrm{st}}}{\mathrm{d}t}=\Delta Q_{\mathrm{in}}+\Delta W_{\mathrm{fw}}\left(\rho_{\mathrm{fw}} h_{\mathrm{fw}}\right)- \\
&\left(X_{\mathrm{tb}} C_{\mathrm{tb0}}+X_{\mathrm{co}} C_{\mathrm{co0}}\right)\left[\left.\frac{\partial\left(h_{\mathrm{st}} \sqrt{\rho_{\mathrm{st}} P_{\mathrm{st}}}\right)}{\partial P_{\mathrm{st}}}\right|_{P_{\mathrm{st0}}}\right] \Delta P_{\mathrm{st}}- \\
&h_{\mathrm{st0}} \sqrt{\rho_{\mathrm{st0}} P_{\mathrm{st0}}}\left(X_{\mathrm{tb}} \Delta C_{\mathrm{tb}}+X_{\mathrm{co}} \Delta C_{\mathrm{co}}\right), \quad (6)
\end{aligned}$$

where $\Delta P_{st}=P_{st}-P_{st0}$, $\Delta W_{fw}=W_{fw}-W_{fw0}$, $\Delta Q_{in}=Q_{in}-Q_{in0}$, $\Delta C_{tb}=C_{tb}-C_{tb0}$ and $\Delta C_{co}=C_{co}-C_{co0}$, and P_{st0}, W_{fw0}, Q_{in0}, C_{tb0} and C_{co0} are the expected steady values of P_{st}, W_{fw}, Q_{in}, C_{tb} and C_{co} at a given power-level, ρ_{st0} and h_{st0} are the steady values of ρ_{st} and h_{st}. Since the steam is saturated, ρ_{st0} and h_{st0} are given by P_{st0}.

Choose the state-vector $\boldsymbol{x}$ and control input u respectively as

$$\boldsymbol{x}=\left[\begin{array}{ll}x_1 & x_2\end{array}\right]^{\mathrm{T}}=\left[\begin{array}{ll}\int_0^t \Delta P_{\mathrm{st}}(\tau) \mathrm{d} \tau & \Delta P_{\mathrm{st}}(t)\end{array}\right]^{\mathrm{T}}, \quad (7)$$

$$u=-\Delta C_{\mathrm{co}}. \quad (8)$$

Then, steam pressure error dynamics (6) can be rewritten as the following state-space model

$$\left\{\begin{array}{l}\dot{x}_1=x_2, \\ \dot{x}_2=-a x_2+b u+d,\end{array}\right. \quad (9)$$

by choosing

$$a=\left\{\frac{V_{\mathrm{s}}}{2}\left[\left.\frac{\partial\left(\rho_{\mathrm{st}} h_{\mathrm{st}}\right)}{\partial P_{\mathrm{st}}}\right|_{P_{\mathrm{st0}}}\right]\right\}^{-1}\left(X_{\mathrm{tb}} C_{\mathrm{tb0}}+X_{\mathrm{co}} C_{\mathrm{co0}}\right)\left[\left.\frac{\partial\left(h_{\mathrm{st}} \sqrt{\rho_{\mathrm{st}} P_{\mathrm{st}}}\right)}{\partial P_{\mathrm{st}}}\right|_{P_{\mathrm{st0}}}\right], \quad (10)$$

$$b=\left\{\frac{V_{\mathrm{s}}}{2}\left[\left.\frac{\partial\left(\rho_{\mathrm{st}} h_{\mathrm{st}}\right)}{\partial P_{\mathrm{st}}}\right|_{P_{\mathrm{st0}}}\right]\right\}^{-1} X_{\mathrm{co}} h_{\mathrm{st0}} \sqrt{\rho_{\mathrm{st0}} P_{\mathrm{st0}}}, \quad (11)$$

$$\begin{aligned}
d=&\left\{\frac{V_{\mathrm{s}}}{2}\left[\left.\frac{\partial\left(\rho_{\mathrm{st}} h_{\mathrm{st}}\right)}{\partial P_{\mathrm{st}}}\right|_{P_{\mathrm{st0}}}\right]\right\}^{-1}\left[\Delta Q_{\mathrm{in}}+\Delta W_{\mathrm{fw}}\left(\rho_{\mathrm{fw}} h_{\mathrm{fw}}\right)-\right. \\
&\left.X_{\mathrm{tb}} h_{\mathrm{st0}} \sqrt{\rho_{\mathrm{st0}} P_{\mathrm{st0}}} \Delta C_{\mathrm{tb}}\right], \quad (12)
\end{aligned}$$

from which it can be seen that a and b are constants, and d is bounded and varied with the operational condition.

2.2 State-Space Model of Grid Frequency

The swing equation of a synchronous generator governing the grid frequency and rotor angle can be expressed as

$$\left\{\begin{array}{l}\dot{\delta}=\omega-1, \\ \dot{\omega}=\dfrac{P_{\mathrm{m}}}{\omega H}-T_{\mathrm{e}},\end{array}\right. \quad (13)$$

where δ is the rotor angle in the synchronously rotating frame, ω is the normalized rotation-rate, H is the mechanical inertia of rotor, P_m is the mechanical power given by the turbine, T_e the electromagnetic torque given by the grid. For a classical multi-machine grid, electromagnetic torque T_e satisfies

$$T_{\mathrm{e}}=G E_{\mathrm{q}}^{\prime 2}+E_{\mathrm{q}}^{\prime} \sum_{k=1}^n \omega_k E_{\mathrm{q}, k}^{\prime}\left(G_k \cos \delta_k+B_k \sin \delta_k\right) \quad (14)$$

where E'_q and G are the voltage and self-conductance of the local generator, δ_k is the rotor angle of the kth remote generator in the local rotating frame, and ω_k, $E'_{q,k}$, G_k and B_k are the rotation-rate, transient voltage, conductance and susceptance of the kth remote generator respectively.

From swing equation (13), the error dynamics of rotor angle and rotation-rate can be given by

$$\left\{\begin{array}{l}\Delta \dot{\delta}=\Delta \omega, \\ \Delta \dot{\omega}=-\dfrac{P_{\mathrm{m}}}{\omega H} \Delta \omega+\dfrac{\Delta P_{\mathrm{m}}}{H}-\Delta T_{\mathrm{e}},\end{array}\right. \quad (15)$$

where $\Delta\delta=\delta-\delta_0$, $\Delta\omega=\omega-\omega_0$, $\Delta P_m=P_m-P_{m0}$, $\Delta T_e=T_e-T_{e0}$, and δ_0, ω_0, P_{m0} and T_{e0} are respectively the setpoints of δ, ω, P_m and T_e with $\omega_0=1$ and $P_{m0}=HT_{e0}$. ΔP_m can be expressed as

$$\Delta P_{\mathrm{m}}=\frac{\Delta G_{\mathrm{tb}}}{G_{\mathrm{tbr}}}+d_{\mathrm{m}}, \quad (16)$$

where constant G_{tbr} is the steam flowrate to the turbine at the rated electrical power-level, $\Delta G_{tb}=G_{tb}-G_{tb0}$, G_{tb0} is the referenced value of G_{tb}, and d_m is a scalar. Based on equation (4),

$$\Delta P_{\mathrm{m}} = \frac{\sqrt{\rho_{\mathrm{st0}} P_{\mathrm{st0}}} X_{\mathrm{tb}}}{G_{\mathrm{tbr}}} \Delta C_{\mathrm{tb}} + \frac{X_{\mathrm{tb}} C_{\mathrm{tb0}}}{G_{\mathrm{tbr}}} \left[\left. \frac{\partial\left(\sqrt{\rho_{\mathrm{st}} P_{\mathrm{st}}}\right)}{\partial P_{\mathrm{st}}} \right|_{P_{\mathrm{st0}}} \right] \Delta P_{\mathrm{st}} + d_{\mathrm{m}} \,. \quad (17)$$

Substitute equations (17) to (15),

$$\begin{cases} \Delta\dot{\delta} = \Delta\omega, \\ \Delta\dot{\omega} = -\dfrac{P_{\mathrm{m}}}{H\omega}\Delta\omega + \dfrac{\sqrt{\rho_{\mathrm{st0}} P_{\mathrm{st0}}} X_{\mathrm{tb}}}{HG_{\mathrm{tbr}}} \Delta C_{\mathrm{tb}} + \\ \quad \dfrac{X_{\mathrm{tb}} C_{\mathrm{tb0}}}{HG_{\mathrm{tbr}}} \left[\left. \dfrac{\partial\left(\sqrt{\rho_{\mathrm{st}} P_{\mathrm{st}}}\right)}{\partial P_{\mathrm{st}}} \right|_{P_{\mathrm{st0}}} \right] \Delta P_{\mathrm{st}} + \dfrac{d_{\mathrm{m}}}{H} - \Delta T_{\mathrm{e}}. \end{cases} \quad (18)$$

By choosing the state-vector $\boldsymbol{x}$ and control input u as

$$\boldsymbol{x} = \begin{bmatrix} x_1 & x_2 \end{bmatrix}^{\mathrm{T}} = \begin{bmatrix} \Delta\delta & \Delta\omega \end{bmatrix}^{\mathrm{T}}, \quad (19)$$

$$u = \Delta C_{\mathrm{tb}}, \quad (20)$$

error dynamics (18) can be also represented as state-space model (9) with constants a and b as well as total disturbance d defined respectively as

$$a = \frac{P_{\mathrm{m0}}}{H}, \quad (21)$$

$$b = \frac{\sqrt{\rho_{\mathrm{st0}} P_{\mathrm{st0}}} X_{\mathrm{tb}}}{HG_{\mathrm{tbr}}}, \quad (22)$$

$$d = \frac{\omega P_{\mathrm{m0}} - P_{\mathrm{m}}}{H\omega}\Delta\omega + \frac{X_{\mathrm{tb}} C_{\mathrm{tb0}}}{HG_{\mathrm{tbr}}} \left[\left. \frac{\partial\left(\sqrt{\rho_{\mathrm{st}} P_{\mathrm{st}}}\right)}{\partial P_{\mathrm{st}}} \right|_{P_{\mathrm{st0}}} \right] \Delta P_{\mathrm{st}} + \frac{d_{\mathrm{m}}}{H} - \Delta T_{\mathrm{e}} \,. \quad (23)$$

2.3 Control Problem Formulation

From state-space model (9), the stabilization problem of both the main steam pressure and grid frequency can be converted to the theoretical control problem summarized as follows.

Problem. Consider the 2nd order dynamical system

$$\dot{\boldsymbol{x}} = \boldsymbol{A}\boldsymbol{x} + \boldsymbol{b}u + \boldsymbol{d} \quad (24)$$

where $\boldsymbol{x}$=[x_1 x_2]$^{\mathrm{T}}$ is the state-vector, u is control input,

$$\boldsymbol{A} = \begin{bmatrix} 0 & 1 \\ 0 & -a \end{bmatrix}, \quad (25)$$

$$\boldsymbol{b} = \begin{bmatrix} 0 & b \end{bmatrix}^{\mathrm{T}}, \quad (26)$$

$$\boldsymbol{d} = \begin{bmatrix} 0 & d \end{bmatrix}^{\mathrm{T}}, \quad (27)$$

both a and b are given positive constants, and d is called total disturbance satisfying

$$\dot{d} = D, \quad (28)$$

where

$$|D| \le M_{\mathrm{d}}, \quad (29)$$

and M_{d} is a bounded positive constant. How to design control input u so that $\boldsymbol{x}\to\Xi$ as $t\to\infty$, where $\boldsymbol{x}$=[x_1, x_2]$^{\mathrm{T}}$ is the state-vector and $\Xi\subset \mathrm{R}^2$ is a bounded set including the origin $\boldsymbol{x}=\boldsymbol{O}$.

3. FLEXIBLE CONTROL BASED ON ACTIVE DISTURBANCE ATTENUATION

From system model (24), it is can be seen that the central in guaranteeing the closed-loop stability is to effectively attenuate total disturbance d. However, from (12) and (23), disturbance d is influenced by many uncertain variables and is impossible to be known accurately, which extensively increase the difficulty in solving the control problem. In this section, instead of modelling the total disturbance, a disturbance observer is given based upon the measurements of system state-vector, and an active disturbance rejection control (ADRC) is then proposed for globally bounded stabilization. This result is summarized as the following theorem.

Theorem. Consider system (24) with state variables measurable. Suppose that total disturbance d satisfies (28) and (29) with positive constant M_{d} being bounded. Then, ADRC

$$u = -b^{-1}\left(k_2 x_1 + k_1 x_2\right) - b^{-1}\hat{d}\,, \quad (30)$$

where k_i>0 (i=1, 2) is the feedback gains, and $\hat{d}$ is the estimation of total disturbance d given by 3rd-order disturbance observer (DO)

$$\begin{cases} \dot{\hat{x}}_1 = \hat{x}_2 - \gamma_1\varepsilon^{-1}e_1 \\ \dot{\hat{x}}_2 = -a\hat{x}_2 + bu + \hat{d} - \gamma_2\varepsilon^{-2}e_1, \\ \dot{\hat{d}} = -\gamma_3\varepsilon^{-3}e_1, \end{cases} \quad (31)$$

with γ_i >0 is the observer gains (i=1, 2, 3), constant $\varepsilon\in(0, 1)$,

$$e_i = \hat{x}_i - x_i, \quad i = 1,2., \quad (32)$$

ADRC (30) can provide globally bounded closed-loop stability if all the roots of algebraic equations

$$s^3 + \left(\gamma_1 + \varepsilon a\right)s^2 + \left(\gamma_2 + \varepsilon a\gamma_1\right)s + \gamma_3 = 0, \quad (33)$$

and

$$s^2 + \left(k_1 + a\right)s + k_2 = 0, \quad (34)$$

have negative real parts.

Proof. First, the convergence of DO (31) is analysed. Define the estimation error of total disturbance d as

$$e_3 = \hat{d} - d\,. \quad (35)$$

Then, from (24), (29) and (31), the observation errors e_i (i=1, 2, 3) satisfy dynamical equation

$$\begin{cases} \dot{e}_1 = -\gamma_1\varepsilon^{-1}e_1 + e_2 \\ \dot{e}_2 = -\gamma_2\varepsilon^{-2}e_1 - ae_2 + e_3, \\ \dot{e}_3 = -\gamma_3\varepsilon^{-3}e_1 - D. \end{cases} \quad (36)$$

Based on coordination transformation

$$\boldsymbol{z} = \begin{bmatrix} z_1 & z_2 & z_3 \end{bmatrix}^{\mathrm{T}} = \begin{bmatrix} e_1 & \varepsilon e_2 & \varepsilon^2 e_3 \end{bmatrix}^{\mathrm{T}} \quad (37)$$

and scale transformation

$$\tau = \varepsilon^{-1}t\,, \quad (38)$$

estimation error dynamics (36) can be rewritten as

$$\frac{\mathrm{d}\boldsymbol{z}}{\mathrm{d}\tau} = \boldsymbol{A}_{\mathrm{o}}\boldsymbol{z} - \varepsilon^3\boldsymbol{D}\,, \quad (39)$$

where

$$\boldsymbol{A}_{\mathrm{o}} = \begin{bmatrix} -\gamma_1 & 1 & 0 \\ -\gamma_2 & -\varepsilon a & 1 \\ -\gamma_3 & 0 & 0 \end{bmatrix}, \quad (40)$$

$$\boldsymbol{D} = \begin{bmatrix} 0 & 0 & D \end{bmatrix}^{\mathrm{T}}. \quad (41)$$

As ε is strictly positive, the stability of error dynamics (36) is equivalent to system (39). Moreover, due to (33) is the characteristic equation of matrix (40), and due to all the roots of (33) have strict negative real parts, for an arbitrarily given positive-definite symmetric matrix $\boldsymbol{Q}_o$, there exists a positive-definite $\boldsymbol{P}_o$ so that Lyapunov equation

$$\boldsymbol{A}_o^T\boldsymbol{P}_o+\boldsymbol{P}_o\boldsymbol{A}_o=-\boldsymbol{Q}_o\,. \tag{42}$$

is well satisfied.

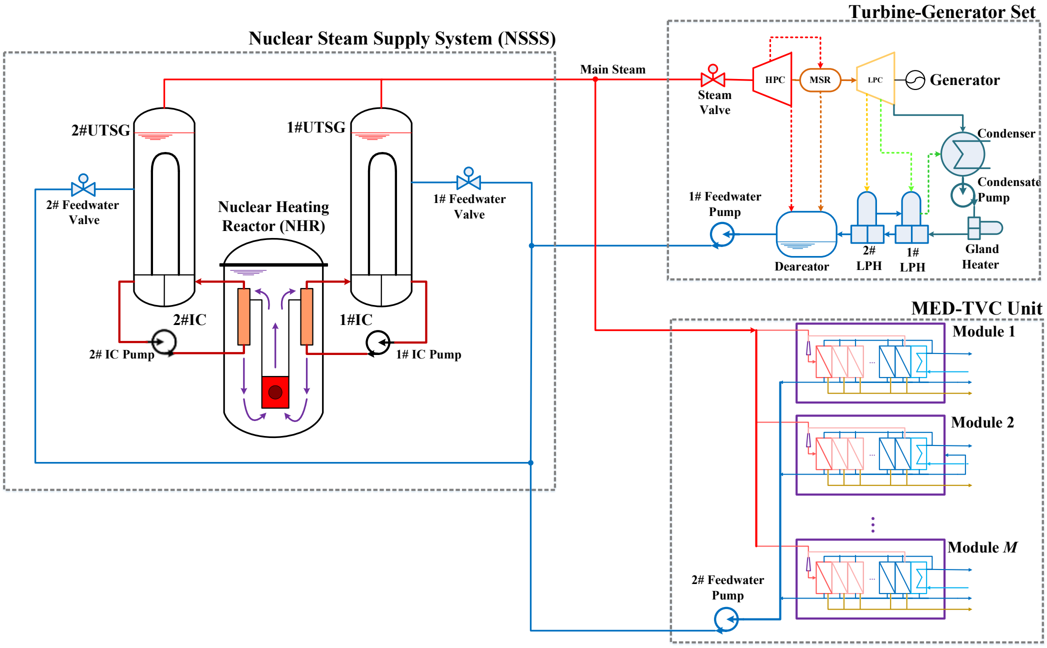

Fig.1. Schematic process diagram of a nuclear heating reactor electricity-water cogeneration plant

From (42), choose the Lyapunov function for system (39) as

$$V_o(z)=\boldsymbol{z}^T\boldsymbol{P}_o\boldsymbol{z}\,, \tag{43}$$

and differentiate V_o along the trajectory of system (39),

$$\begin{aligned}\frac{\mathrm{d}V_o(z)}{\mathrm{d}\tau}&=2z^T\boldsymbol{P}_o\left(\boldsymbol{A}_o z-\varepsilon^3\boldsymbol{D}\right)\\&=z^T\left(\boldsymbol{P}_o\boldsymbol{A}_o+\boldsymbol{A}_o^T\boldsymbol{P}_o\right)z-2\varepsilon^3 z^T\boldsymbol{P}_o\boldsymbol{D}\\&\le-\frac{1}{2}z^T\boldsymbol{Q}_o z+2\varepsilon^6\boldsymbol{D}^T\boldsymbol{P}_o\boldsymbol{Q}_o^{-1}\boldsymbol{P}_o\boldsymbol{D}.\end{aligned} \tag{44}$$

From inequality (44), vector z converges globally and asymptotically to a bounded set around the origin, which means that DO (31) provides a globally bounded estimation of total disturbance d. It can be also seen that if constant ε is smaller and the real parts of the roots of (34) are more negative, then the bounded set around the origin is tighter.

Second, the stability of closed-loop system constitued by (24) , (30) and (31) is analyzed. From equation (24) and (30), the closed-loop dynamics can be written as

$$\dot{\boldsymbol{x}}=\boldsymbol{A}_c\boldsymbol{x}-\boldsymbol{E}_d\,, \tag{45}$$

where

$$\boldsymbol{A}_c=\begin{bmatrix}0 & 1\\ -k_2 & -(k_1+a)\end{bmatrix}, \tag{46}$$

$$\boldsymbol{E}_d=\begin{bmatrix}0 & e_3\end{bmatrix}^T. \tag{47}$$

Since gains k_1 and k_2 are chosen so that both the two roots of algebraic equation (34) have strict real parts, for an arbitrarily given positive-definite symmetric matrix $\boldsymbol{Q}_c$, there exists a positive-definite matrix $\boldsymbol{P}_c$ satisfying Lyapunov equation

$$\boldsymbol{A}_c^T\boldsymbol{P}_c+\boldsymbol{P}_c\boldsymbol{A}_c=-\boldsymbol{Q}_c\,. \tag{48}$$

Then, choose Lyapunov function of system (45) as

$$V_c(\boldsymbol{x})=\boldsymbol{x}^T\boldsymbol{P}_c\boldsymbol{x}\,, \tag{49}$$

and differentiate function V_c along the trajectory of (45),

$$\begin{aligned}\dot{V}_c(\boldsymbol{x})&=2\boldsymbol{x}^T\boldsymbol{P}_c\left(\boldsymbol{A}_c\boldsymbol{x}-\boldsymbol{E}_d\right)\\&=\boldsymbol{x}^T\left(\boldsymbol{A}_c^T\boldsymbol{P}_c+\boldsymbol{P}_c\boldsymbol{A}_c\right)\boldsymbol{x}-2\boldsymbol{x}^T\boldsymbol{P}_c\boldsymbol{E}_d\\&\le-\frac{1}{2}\boldsymbol{x}^T\boldsymbol{Q}_c\boldsymbol{x}+2\left(\boldsymbol{\eta}^T\boldsymbol{P}_c\boldsymbol{Q}_c^{-1}\boldsymbol{P}_c\boldsymbol{\eta}\right)e_3^2,\end{aligned} \tag{50}$$

where $\boldsymbol{\eta}=\begin{bmatrix}0 & 1\end{bmatrix}^T$.

From the performance analysis of DO (31), disturbance estimation error e_3 can be arbitrarily small by properly choosing ε. Hence, from inequality (50), state $\boldsymbol{x}$ converges globally and asymptotically to a bounded set around the origin. The proof is completed.

Remark. From system model (24), it can be seen that ADRC (30) can be rewritten as

$$u=-\frac{1}{b}\left[k_1x_2+k_2\int_0^t x_2(\tau)\,\mathrm{d}\tau\right]-\frac{\hat{d}}{b}, \tag{51}$$

which is an addition of a proportional-integral (PI) feedback action and a feedforward action driven by DO (31).

4. APPLICATION TO A NHR COGENERATION PLANT

4.1 The NHR Cogeneration plant and its Control System

The schematic process diagram of the nuclear heating reactor (NHR) plant cogenerating electricity and desalinated water is shown in Fig. 1. This NCP is mainly composed of a NSSS, a turbine-generator set and a MED-TVC desalination process, where the NSSS is further composed of a 200MW$_t$ NHR, two forced-circulated intermediate circuits (ICs) and two U-tube steam generators (UTSGs) giving saturated live steam (Dong, Pan, 2018). The heat is transferred from the reactor to steam generators via two ICs, and converts the feedwater to saturated live steam. The live steam flows from the two UTSGs are combined to form the main steam flow which is then distributed to both the turbine and MED-TVC modules for electricity generation and seawater desalination.

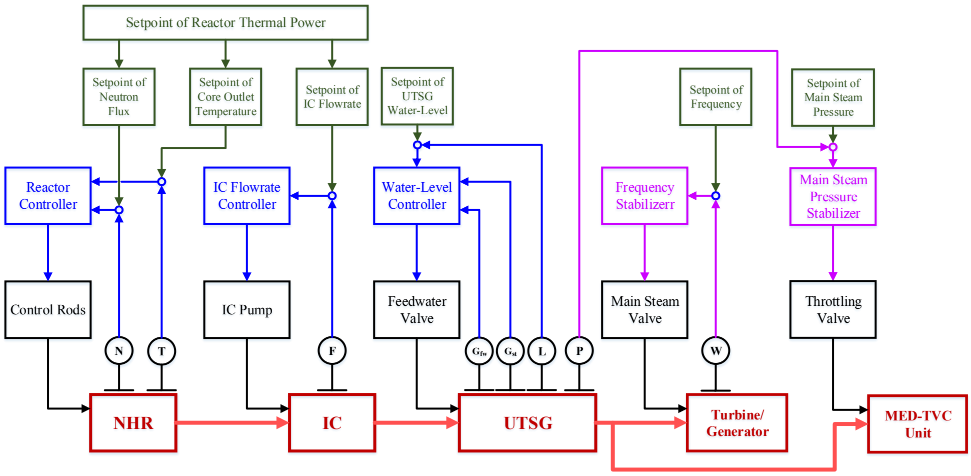

Fig. 2. Flexible control scheme of NHR cogeneration plant

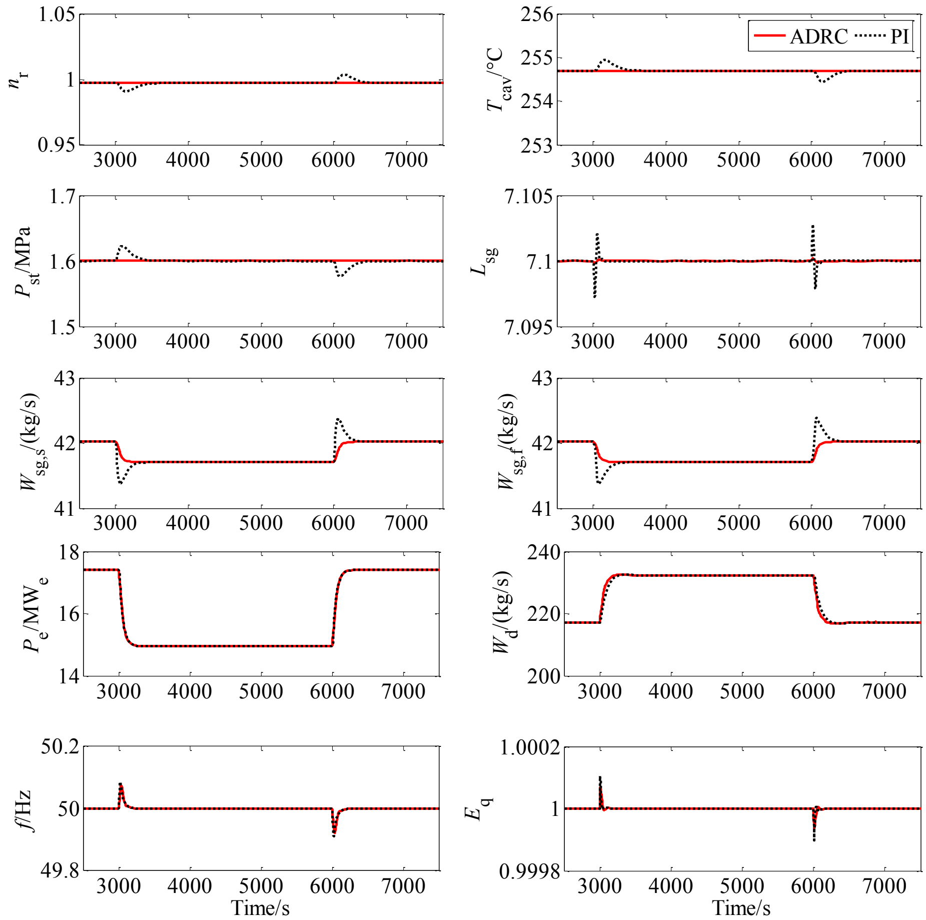

Fig. 3. Simulation results in the case of load stepping, n_r: neutron flux, T_{cav}: average temperature of primary coolant, P_{st}: main steam pressure, L_{sg}: UTSG water-level, $W_{sg,s}$: main steam flowrate, $W_{sg,f}$: feedwater flowrate, P_e: electric power, W_d: product of potable water, f: grid frequency, and E_q: normalized voltage.

The coordinated control system of NHR cogeneration plant is schematically illustrated in Fig. 2. The NSSS control system is constituted by the reactor controller, IC flowrate controller and water-level controller, which generates the driving signal of control rods, IC pumps and feedwater valves based on the setpoints and measurements of neutron flux, core outlet temperature, IC flowrates and UTSG water-levels. The regulation algorithms of NSSS control systems adopts the classical proportional-differential-integral (PID) feedback laws presented in (Dong, 2013; Dong, et al. 2009). The flexible control system is formed by the frequency stabilizer and the main steam pressure stabilizer which adopt the ADRC given in Section 3 as control algorithm to generate the expected openning of the main steam valve of turbine and the expected ejector nozzle cross-section area of every MED-TVC module.

4.2 Simulation Result

To show the feasibility of ADRC (30) in the flexible control of NHR cogeneration plant, numerical simulation is done on Matlab/Simulink platform. In the simulation, the performance of ADRC (30) is compared with that of the PI control given by equation (51) without the last term driven by the disturbance estimation are compared with each other. The case considered in this simulation is load stepping: Initially, the NHR operates at its rated power, where 70% of maim steam flow are used for electricity generation. At 3000s, a load in the grid steps down with an amplitude of $2.5MW_e$, and the load steps back up to its original level at 6000s. The transient responses of some key process variables are shown in Fig. 3.

4.3 Discussions

From Fig. 3, when the electric load steps down, the grid frequency increases quickly, which drives the frequency stabilizer to decrease the opening of main steam regulating valve at the inlet of turbine so as to maintain power balance. As the electric power balance is reached, the frequency returns to its setpoint. The smaller opening of turbine steam valve leads to the increase of steam pressure, which is further suppressed by the main steam pressure stabilizer via enlarging the cross-section area of ejector nozzles in MED-TVC modules.

From Fig. 3, though both the ADRC and PI control can keep the balance of power and heat, the difference between the two control strategies in the aspect of control performance is apparent. The overshoots of neutron flux, primary coolant temperature, main steam pressure and UTSG water-level induced by the ADRC is much smaller than those induced by the classical PI controller. The overshoot of grid frequency during load stepping given by the ADRC is smaller than that given by the PI controller. Moreover, since the overshoot of terminal voltage corresponding to the ADRC is smaller than that corresponding to the PI in both the cases of load stepping and ramping, it can be seen that ADRC can induce a slower frequency variation rate. Actually, the difference in the control performance is induced by the feedforward term, i.e. the last term in (51) given by the total disturbance estimation from DO (31). The total disturbance d can induce a stronger deviation in the process variables if there is no feedforward term attenuating the disturbance actively. The effectiveness of DO (31) is manifested by the higher performance of ADRC which relies on the convergence of disturbance estimation.

In a summary, with comparison to the classical PI algorithm, the ADRC (51) can keep a better balance between the supply and consumption of power and heat. Moreover, since DO (31) can easily realized by a program on any digital control system platforms, ADRC (51) is practically implementable.

5. CONCLUSIONS

To suppress the grid fluctuation caused by the IRE generation, it is necessary to study the flexible control of NCPs, whose central problem is to redistribute the main steam between the turbine and cogeneration process according to IRE generation. In this paper, a flexible control strategy of NCPs with saturated main steam is newly proposed based upon the idea of active disturbance attenuation. The flexibility is realized by the stabilization of grid frequency and main steam pressure through main steam flow redistribution, where the stabilization is further transferred to the disturbance attenuation of a 2^{nd}-order dynamical system. Then, an ADRC is originally designed for realizing disturbance attenuation, where the disturbance estimation is provided by a novel 3^{rd}-order DO. Finally, this newly-built ADRC is applied to the flexible control of a NCP composed of a NHR, a turbine-generator set and a MED-TVC seawater desalination process, and numerical simulation results show that the flexibility of this NCP is satisfactorily guaranteed by the flexible control strategy for grid balancing.

REFERENCES

Alizadeh, M.I., Moghaddam, M.P., Amjady, N., Siano, P., Sheikh-El-Eslami M.K. (2016). Flexibility in future power systems with high renewable penetration: A review. *Renewable and Sustainable Energy Reviews*, 57, 1186-1193.

Cany, C., Mansilla, C., da Costa, P., Mathonnière, G., Duquesnoy, T., Baschwitz, A. (2016). Nuclear and intermittent renewables: Two compatible supply options? The case of the French power mix. *Energy Policy*, 95, 135-46.

Dong, Z., Pan, Y. (2018). A lumped-parameter dynamical model of a nuclear heating reactor cogeneration plant. *Energy*, 145, 638-656.

Dong, Z. (2013). PD power-level control design for PWRs: a physically-based approach. *IEEE Transactions on Nuclear Science*, 60, 3889-98.

Dong, Z., Huang, X., Feng, J. (2009). Water-level control for the U-tube steam generator of nuclear power plants based on output feedback dissipation. *IEEE Transactions on Nuclear Science*, 56, 1600-1612.

Kondziella, H., Bruckner, T. (2016). Flexibility requirements of renewable energy based electricity systems – a review of research results and methodologies. *Renewable and Sustainable Energy Reviews*, 53, 10-22.

Li, G., Wang, X., Liang, B., Li, X., Zhang, B., Zou, Y. (2016). Modeling and control of nuclear reactor cores for electricity generation: A review of advanced technology. *Renewable and Sustainable Energy Reviews*, 60, 116-128.

Locatelli, G., Fiordaliso, A., Boarin, S., Ricotti, M.E. (2017). Cogeneration: An option to facilitate load following in small modular reactors. *Progress in Nuclear Energy*, 97, 153-161.

Lund, P. D., Lindgren, J., Mikkola, J., Salpakari, J. (2015) Review of energy system flexibility measures to enable high levels of variable renewable electricity. *Renewable and Sustainable Energy Review*s, 45, 785-807.

Suman, S. (2018). Hybrid nuclear-renewable energy systems: A review. *Journal of Cleaner Production*, 181, 166-177.